Acta Pharmaceutica Sinica B 2024;14(8):3561−3575

Chinese Pharmaceutical Association
Institute of Materia Medica, Chinese Academy of Medical Sciences

Acta Pharmaceutica Sinica B

www.elsevier.com/locate/apsb
www.sciencedirect.com

ORIGINAL ARTICLE

Small molecule α-methylene-γ-butyrolactone, an evolutionarily conserved moiety in sesquiterpene lactones, ameliorates arthritic phenotype *via* interference DNA binding activity of NF-κB

Kegang Linghu[a,b,d,†], Wenqing Cui[b,†], Taiqin Li[b,†], Yueting Tuo[b], Dasong Wang[b], Huiqi Pan[b], Tian Zhang[c,d], Ligen Lin[c], Hua Yu[c], Xiaoxia Hu[b,*], Haiyang Li[a,d,*], Xiangchun Shen[b,*]

[a]*Department of Surgery, the Affiliated Hospital of Guizhou Medical University, Guiyang 550001, China*
[b]*The Key Laboratory of Optimal Utilization of Natural Medicine Resources, School of Pharmaceutical Sciences, Guizhou Medical University, Guian New District, Guizhou 561113, China*
[c]*State Key Laboratory of Quality Research in Chinese Medicine, Institute of Chinese Medical Sciences, University of Macau, Macao SAR 999078, China*
[d]*Guizhou Institute of Precision Medicine, Affiliated Hospital of Guizhou Medical University, Guiyang 550001, China*

Received 29 December 2023; received in revised form 3 March 2024; accepted 27 March 2024

KEY WORDS

α-Methylene-γ-butyrolactone;
Rheumatoid arthritis;
NF-κB p65;
Synovial microenvironment;
Sesquiterpene lactones

Abstract Rheumatoid arthritis (RA) is an inflammatory disease accompanied by abnormal synovial microenvironment (SM). Sesquiterpene lactones (SLs) are the main anti-inflammatory ingredients of many traditional herbs utilized in RA treatment. α-Methylene-γ-butyrolactone (α-M-γ-B) is a core moiety that widely exists in natural SLs. This study was designed to investigate the anti-arthritic potential of α-M-γ-B as an independent small molecule *in vitro* and *in vivo*. α-M-γ-B exhibited stronger electrophilicity and anti-inflammatory effects than the other six analogs. α-M-γ-B inhibited the production of pro-inflammatory mediators *via* repolarizing M1 macrophages into M2 macrophages. The transcriptome sequencing suggested that α-M-γ-B regulated the immune system pathway. Consistently, α-M-γ-B attenuated collagen type II-induced arthritic (CIA) phenotype, restored the balance of Tregs-macrophages and remodeled SM *via* repolarizing the synovial-associated macrophages in CIA mice. Mechanistically, although α-M-γ-B did not prevent the trans-nucleus of NF-κB it interfered

*Corresponding authors.
E-mail addresses: hxx@gmc.edu.cn (Xiaoxia Hu), lihaiyang@gmc.edu.cn (Haiyang Li), shenxiangchun@126.com (Xiangchun Shen).
[†]These authors made equal contributions to this work.
Peer review under the responsibility of Chinese Pharmaceutical Association and Institute of Materia Medica, Chinese Academy of Medical Sciences.

https://doi.org/10.1016/j.apsb.2024.04.004

with the DNA binding activity of NF-κB *via* direct interaction with the sulfhydryl in cysteine residue of NF-κB p65, which blocked the activation of NF-κB. Inhibition of NF-κB reduced the M1 polarization of macrophage and suppressed the synovial hyperplasia and angiogenesis. α-M-γ-B failed to ameliorate CIA in the presence of *N*-acetylcysteine or when the mice were subjected to the macrophage-specific deficiency of *Rela*. In conclusion, α-M-γ-B significantly attenuated the CIA phenotype by directly targeting NF-κB p65 and inhibiting its DNA binding ability. These results suggest that α-M-γ-B has the potential to serve as an alternative candidate for treating RA. The greater electrophilicity of α-M-γ-B, the basis for triggering strong anti-inflammatory activity, accounts for the reason why α-M-γ-B is evolutionarily conserved in the SLs by medical plants.

1. Introduction

Rheumatoid arthritis (RA) is a prevalent autoimmune disorder characterized by aberrant inflammatory synovial hyperplasia, angiogenesis, and irreversible destruction of cartilage and bone[1]. So far, approximately 1%−2% of the global population is deeply troubled by RA, which seriously affects people's health and life quality[2]. Currently employed conventional medications (such as NSAIDs, DMARDs, and glucocorticoids) could not cure RA completely or be linked with significant adverse effects[3]. Therefore, seeking available targets and potential therapeutic candidates is important for RA treatment.

Growing findings have indicated a strong correlation between the synovial microenvironment (SM) and the pathological progression of RA[4]. Macrophages, fibroblast-like synoviocytes, and vascular endothelial cells constitute the primary cell members of the SM in RA joints[5]. Among the three cell types involved in SM, macrophages play a crucial role. Macrophages possess the ability to polarize into distinct phenotypes, namely M1 and M2, depending on the stimuli they encounter. The presence of M1 macrophages initiates an early inflammatory response by producing pro-inflammatory cytokines. Conversely, M2 macrophages secret anti-inflammatory cytokines like IL-10. Studies have shown that an increased M1/M2 ratio could break the dynamic balance of SM in the joint, which promotes RA progression by triggering angiogenesis and synovial hyperplasia[6]. Therefore, seeking effective targets and therapeutic candidates to repolarize M1 macrophages into M2 macrophages would be an encouraging approach for managing RA.

NF-κB represents a canonical signaling pathway implicated in the regulation of M1 macrophage polarization and has been widely acknowledged as the primary inflammatory pathway involved in RA[7]. Several RA treatment drugs were reported to ameliorate RA *via* regulating NF-κB[8]. Under basal conditions, IκBα (a NF-κB inhibitor) binds with NF-κB dimer (p65−p50) and confines NF-κB within the cytoplasm. Upon receiving inflammatory stimulation, the IκB kinase complex (IKKγ, IKKβ, and IKKα) promptly phosphorylates IκBα which then undergoes proteasome-mediated disruption. Subsequently, the NF-κB dimer moves towards the nucleus and physically interacts with DNA to facilitate the transcription and translation of pro-inflammatory genes, which promotes the M1 macrophage polarization and inflammatory cytokine cascade, leading to the onset and deterioration of RA[7]. Hence, the nucleus entry of NF-κB and its physical interaction with DNA represent the pivotal stage in the activation process of NF-κB. Interference of NF-κB's DNA binding activity is deemed to be a potential therapeutic strategy for RA treatment.

Sesquiterpene lactones (SLs) represent the principal bioactive constituents of various traditional herbs belonging to the Asteraceae[9]. They have been acknowledged for their remarkable anti-inflammatory activities in different inflammation models[10,11]. However, the complex purification route and low content limit the development and application of SLs[12]. Previous studies indicated that α,β-unsaturated ketone moiety widely existed in the anti-inflammatory SLs. Helenalin, a natural SL and a commercial NF-κB inhibitor, was reported to inhibit inflammation through the presence of two α,β-unsaturated active groups[13]. Our previous work demonstrated that Leocarpinolide B, a kind of SL with the α,β-unsaturated ketone moiety, showed great potential for anti-inflammation and anti-RA treatment[14,15]. Based on the most significant characteristics of SLs with the conserved moiety of α-methylene-γ-butyrolactone (α-M-γ-B) which embodies typical α,β-unsaturated ketone moiety, we obtained the SLs-structure-simplified small molecule α-M-γ-B. The present study was designed to elucidate the anti-inflammatory and anti-arthritic potentials of small molecule α-M-γ-B independent of the parent structure of SLs.

Our findings demonstrated that the α-M-γ-B effectively attenuated the arthritic phenotype induced by collagen type II in mice by directly targeting NF-κB p65 and inhibiting its DNA binding activity. The greater electrophilicity of α-M-γ-B, the basis for triggering strong anti-inflammatory activity, accounts for the reason why α-M-γ-B is evolutionarily conserved in the SLs by medical plants.

2. Materials and methods

2.1. Materials

Chemical and biological materials used in this study were listed in Supporting Information Table S1.

2.2. Cell culture

Human SW982 synovial cells were obtained from Procell (Wuhan, China). Mouse RAW264.7 and human THP-1 cells were procured from the ATCC (Manassas, VA, USA). Vascular endothelial cell HUVEC was obtained from ScienCell (San Diego, CA,

USA). SW982 and RAW264.7 cells were incubated in DMEM (basal medium, 10% FBS, and 1% P/S) with an atmosphere of 5% CO_2 and 95% humidity at 37 °C. Human THP-1 cells were cultured in RPMI 1640. THP-1 cells were subjected to stimulation with 100 ng/mL PMA for 12 h to differentiate into macrophages. HUVEC was cultured in an endothelial cell medium (basal medium, 5% FBS, 1% P/S, and 1% growth supplement factor). Bone marrow-derived macrophages (BMDMs) were derived from the mice and cultured according to a previously established protocol[16].

2.3. Assessment of cellular viability

The cellular viability of RAW264.7 cells and PMA-induced THP-1 macrophages was performed by MTT assay according to a previously established protocol[17].

2.4. Determination of nitric oxide (NO)

The NO in the collected culture supernatant was determined with the previously established Greiss reagent method[14].

2.5. Enzyme-linked immunosorbent assay (ELISA)

C-reactive protein (CRP), cytokines, and autoantibodies in cell culture supernatants or mouse serum were conducted with commercial ELISA kits, following the manufacturer's instructions.

2.6. Transcriptome sequencing

BMDMs were isolated from the mice and grew to 90% confluence, then cells were incubated with α-M-γ-B (6 μmol/L) for 6 h. Subsequently, precooled PBS was used to wash the cells twice. Then BMDMs were lysed with Trizol reagent. The resulting lysates were subjected to sequencing for comprehensive transcriptome analysis.

2.7. Synovial cell assays (proliferation, migration, and invasion)

THP-1 was co-incubated with α-M-γ-B along with or without LPS stimulation for 12 h. After removing the medium, THP-1 macrophages were rinsed with PBS and subsequently with fresh medium for an additional 12 h. The culture medium was gathered and centrifugated for 5 min at 1200 rpm, followed by harvesting the supernatant as macrophage-conditioned media (MCM). To simulate the impact of synovial-associated macrophages on the synovial microenvironment, we used the MCM to treat the synovial cells and detect their proliferation, migration, and invasion.

Scratch wound healing assay was employed to detect the proliferation and migration of synovial cells. Specifically, the SW982 synovial cells were seeded and cultured until reaching confluence. Subsequently, a sterile pipette tip was employed to create a scratch wound in each well. The SW982 synovial cells were subsequently exposed to MCM for 0 or 24 h, then photographs were obtained by an inverted microscope (Leica, Wetzlar, Germany).

The effects of α-M-γ-B on the invasion of synovial cells were evaluated using a transwell chamber (NEST, China) supplemented with an extracellular matrix gel (MCE, USA) before introducing cells into the upper chamber[18]. SW982 cells were administered with MCM for 12 h. Subsequently, SW982 cells were suspended in a medium without FBS and added into the upper layer. The lower chamber was supplemented with 600 mL of DMEM containing 10% FBS. After an 8-h incubation, non-migrated cells were gently removed. Finally, the membrane was fixed with a 4% polyformaldehyde solution for 20 min and stained with DAPI. The SW982 cells towards the undersurface of the membrane were quantified under a fluorescence microscope (Leica, Wetzlar, Germany).

2.8. Adhesion assay of monocytes to synovial cells

THP-1 monocytes were labeled with 5 μmol/L BCECF/AM in RPMI-1640 medium for 40 min. Then labeled THP-1 monocytes were collected through centrifugation and subjected to thrice PBS washing. SW982 cells were co-treated with MCM established in method 2.7 for 12 h and then subjected to twice PBS washing. The treated SW982 cells were incubated with 1×10^5 BCECF/AM-labelled THP-1 monocytes/well for 1 h. Subsequently, the unattached THP-1 cells were eliminated through PBS washing. Fluorescent images were obtained through fluorescent microscopy (Leica, Wetzlar, Germany).

2.9. Tube formation assay

To evaluate the impact of α-M-γ-B on the angiogenesis of vascular endothelial cells in the synovial microenvironment, HUVECs were subjected to treatment with MCM established in method 2.7 for 6 h, then the HUVECs were seeded with 50 μL of Matrigel in a 96-well plate. Tube formation was observed under an inverted microscope 8 h later. The formation of tube junctions was meticulously recorded using the angiogenesis analysis plugin within the ImageJ software.

2.10. Flow cytometry

RAW264.7 cells were seeded for growth overnight. Cells were pretreated with α-M-γ-B (3, 6, 12 μmol/L) for 1 h, then followed by co-treatment with 200 ng/mL LPS for 12 h. Then the cells were stained with dichlorodihydrofluorescein diacetate (DCFH-DA), Arginase 1, or CD86 at the recommended concentrations for 30 min at 4 °C. Following triple PBS washes, a flow cytometer (Agilent Technologies, CA, USA) was used to quantify the stained cells. The $CD4^+Foxp3^+$ lymphocytes analysis in the immune organs was performed as our previously reported methods[18].

2.11. Immunofluorescence

RAW264.7 cells were seeded on confocal chambers (NEST, Shanghai, China) overnight. Then cells were pretreated with 12 μmol/L α-M-γ-B or 1 mmol/L sulfasalazine (SSZ) for 1 h, followed by 1 h LPS stimulation. The procedures of immunofluorescence staining were conducted as our previously reported method[14].

Paraffin sections of synovial tissues were processed for immunofluorescent staining unitizing antibodies against F4/80 (1:100), CD86 (1:100), H-type vessels marker CD31 and EMCN (1:100), synovial fibroblast marker MMP3 and Vimentin (1:100). The experimental details were reference to our previous reports[18].

2.12. Western blot analysis

The expression of proteins was determined through Western blot analysis employing previously established methodologies[14].

2.13. Quantitative real-time PCR (qPCR) analysis

RNA total extraction was isolated from cells or tissues utilizing the RNA-easy isolation reagent (Vazyme, Nanjing, China), then converted into complementary DNA (cDNA) employing the reverse transcription kit. The amplification of cDNA was performed by SYBR kit, reference to our reported running program[17]. Primer sequences were listed in Supporting Information Table S2.

2.14. Molecular docking between α-M-γ-B and IκBα-NF-κB p65-NF-κB p50 protein complex

3D crystal structure of IκBα-NF-κB p65-NF-κB p50 protein complex (PDBID: 1NFI) was obtained from the PDB database. The small molecule ligand was assigned as the ligand and the 1NFI protein was assigned as the receptor. Pymol software was used to remove the original water molecules in the 3D crystal structure. Subsequently, AutodockTools (http://mgltools.scripps.edu/downloads) was utilized to perform receptor hydrogenation, charge calculation, and generate.pdbqt files. AutoDock Vina 1.1.2 was used for conformation searching and scoring with a searching box placed to include all the surfaces of the receptor to find the optimal binding site. Discovery Studio software was used to visualize the interaction map.

2.15. NF-κB p65 binding activity assay

RAW264.7 was cultured on 100 mm dishes and incubated with 12 μmol/L α-M-γ-B for 1 h before LPS stimulation. Cytoplasmic and nuclear proteins in the RAW264.7 macrophages or the synovial tissue from CIA mice were extracted following the procedures of a commercially available kit. Finally, NF-κB p65 binding activity was assessed with a transcription factor assay kit following the manufacturer's instructions.

2.16. Cellular thermal shift assay (CETSA)

The RAW264.7 cell was lysed in RIPA lysis buffer. Then the cell lysates were allocated for 20 min centrifugation at 4 °C. The protein was quantified (3 μg/μL) and aliquoted into new centrifuge tubes, followed by 3 min boiling at different temperatures (51, 54, 57, 60, 63, 66, 69, 72, 75, 78 °C), using a thermal mixer. Then the lysates were subjected to centrifugation (12,000 rpm, 20 min, 4 °C). Finally, the supernatants were subjected to 95 °C heating with 5× loading buffer before blot analysis.

2.17. Isothermal titration calorimetry (ITC)

This experiment was performed on a MicroCal PEAQ-ITC isothermal titration calorimeter as the manufacturer's indicated procedures (Malvern Panalytical Ltd., Malvern, UK). Briefly, α-M-γ-B (10 μmol/L) was titrated at constant temperature into a pool containing NF-κB p65 protein (100 μmol/L), and the heat released by binding was recorded in real-time. A binding curve was obtained by comparing the thermal effect produced by each titration to the mole of the titration and the titrated molecule.

2.18. Electrophoretic mobility shift assays (EMSA)

This assay was performed unitizing the EMSA kit according to the directions. Briefly, nuclear protein extracts from RAW264.7 macrophages or the synovial tissue from CIA mice were isolated using a nuclear protein extraction kit. The nuclear protein and biotin-labeled DNA probe were co-incubated for 20 min, and the non-binding probe was separated on the non-denatured polypropylene gel electrophoresis. NF-κB consensus oligonucleotide: 5′-AGT TGA GGG GAC TTT CCC AGG C-3′, 3′-TCA ACT CCC CTG AAA GGG TCC G-5′.

2.19. Chromatin immunoprecipitation (ChIP)

The purpose of this assay was to assess the inhibitory effect of α-M-γ-B on the binding capacity of NF-κB p65 to the DNA related to M1 polarization (*NOS2* promoter) and inflammation (*IL6* promoter). THP-1 macrophages were cultured overnight in 100 mm culture dishes, followed by co-treatment with α-M-γ-B (12 μmol/L) and LPS (100 ng/mL). ChIP assay was performed in the treated THP-1 macrophages following the manufacturer's procedures. The primary antibodies were listed in Table S1 and qPCR primers were listed in Table S2.

2.20. Binding analysis between α-M-γ-B and sulfhydryl group

α-M-γ-B were solubilized in methanol with *N*-acetylcysteine (NAC) or glutathione (GSH) for 12 h. Subsequently, the covalent binding between the α-M-γ-B and sulfhydryl group on NAC or GSH was identified unitizing a previously established UPLC−MS system (Waters Corp., Milford, USA)[17]. The sample volume per injection was 5 μL and eluted with the mobile phase consisting of water:acetonitrile:formic acid (81:19:0.1, *v*/*v*/*v*), at a flow rate of 0.4 mL/min.

2.21. Animals and acute toxicity observation of α-M-γ-B

Adult Balb/c male mice, 7−8 weeks, were supplied by Guizhou Laboratory Animal Engineering Technology Center, Guizhou Medical University. The mice were maintained under a controlled laboratory setting[18]. The experimental procedures involving animals were granted approval by the experimental animal ethics committee at Guizhou Medical University (document No.: 2200450). The animal experiments were conducted in compliance with the authorized guidelines and regulations.

Twelve mice were randomly assigned into two experimental groups: Ctrl (Control), 100 mg/kg of α-M-γ-B. The mice were intraperitoneally injected once daily. On Day 7, the mice were sacrificed by implementing CO_2 inhalation. Blood chemistry assays (alkaline phosphatase, aspartate transaminase, and alanine transaminase; ALP, AST, and ALT) were conducted by unitizing the testing kits. Moreover, the kidney, liver, and lung were subjected to histopathological inspection using hematoxylin−eosin (H&E).

2.22. Establishment of NF-κB p65 knockdown, collagen-induced arthritis, and drug treatment

To establish the macrophage-specific knockdown of NF-κB p65 (*Rela*) in mice, adeno-associated virus (AAV) vector with the macrophage-specific promoter F4/80-mediated knockdown of mouse *Rela* (AAV-F4/80-MCS-GDGreen-miR30 shRNA (*Rela*)-WPRE) and control (AAV-F4/80-MCS-GDGreen-WPRE) were supplied by OBiO Biotechnology (Shanghai, China). Knockdown efficiency of *Rela* in peritoneal macrophages and BMDMs was verified on the thirtieth day, then mice were subjected to the CIA model and drug treatment.

The collagen-induced arthritis (CIA) was reproduced by employing bovine type II collagen (CII) emulsified in incomplete Freund's adjuvant (ICFA). For the anti-arthritic investigation of α-M-γ-B, mice were subjected to random allocation to 6 groups (n = 6 in each): Ctrl (Control), CIA (model), CIA-α-M-γ-B (2.5, 5 and 10 mg/kg) and CIA−dexamethasone (DEX). For the mechanisms of α-M-γ-B on anti-arthritis, mice were allocated into 7 groups randomly (n = 5 in each): Vehicle, CIA (model), CIA+α-M-γ-B (10 mg/kg), CIA+α-M-γ-B (10 mg/kg) + NAC (20 mg/kg), CIA + Ad-scramble, CIA + Ad-sh-*Rela* and CIA + Ad-sh-*Rela*+α-M-γ-B (10 mg/kg). The experimental mice were subjected to intraperitoneal injections (saline or the indicated drugs, once daily) for 19 days. The body weights were recorded, and the clinical signs of RA were assessed every other day following previously described methods[18]. Finally, mice were euthanized by CO_2 inhalation, serum was separated for ELISA, the lymphocytes from the spleen, thymus, and lymph nodes were isolated for the flow cytometry analysis, the synovial tissues were dissected to conduct the qPCR and immunofluorescence—the rest hind paw tissues after required experiments were preserved at −80 °C for subsequent analysis.

2.23. *Arthritis score, radiographic and histopathological evaluation*

The severity of arthritis in both hind paws was assessed once every two days after the primary immunization. Assessment of arthritis score was performed according to the reported methods[15]. The arthritis score was determined by summing up the scores of both hind paws, with a maximum score of 8 per mouse. On the last day of the experiment, hind paw plain films were acquired using the imaging system (Clipper, MA, USA). The hind limbs were decalcified according to the established protocol and subsequently subjected to histopathological analysis[18].

2.24. *Statistical analysis*

Results from these experiments were presented as the mean ± SD based on a minimum of three independent tests. GraphPad Prism 6.0 was employed for data analysis. Significant differences between groups were accomplished by performing a one-way analysis of variance, followed by Dunnett's multiple comparisons test. Significance was set at $P < 0.05$. 'NS' stands for non-significance.

3. Results

3.1. *α-M-γ-B is a conserved moiety in natural SLs with anti-inflammatory activity*

There are more than 5000 reported structures of sesquiterpene lactones (SLs), which are sorted into various skeletal subtypes[10,12]. As shown in Fig. 1A and Supporting Information Table S3, we summarized the main skeletal subtypes of SLs with anti-inflammatory activity, including germacranolides, guaianolides, eudesmanolides, heliangolides, and pseudoguaianolides. Interestingly, almost all anti-inflammatory SLs embodied a core α-methylene-γ-butyrolactone (α-M-γ-B) moiety (marked with blue in Fig. 1B), suggesting that α-M-γ-B is a conserved moiety existed in anti-inflammatory SLs.

Inspired by the characteristic of anti-inflammatory SLs with the conserved α-M-γ-B, we obtained the SLs-structure-simplified small molecule α-M-γ-B (Fig. 1C) and other six analogs (Fig. 1D) including 3-methylenetetrahydro-2*H*-pyran-2-one (3M2P2O), 2(5*H*)-furanone (2F), 2-cyclopenten-1-one (2CO), γ-methylene-γ-butyrolactone (γ-M-γ-B), α-methyl-γ-butyrolactone (α-M-γ-B-1) and γ-butyrolactone (γ-B). Among the six analogs, 3M2P2O, 2F, and 2CO were occasionally reported to be independently embodied in the chemical structures of anti-inflammatory SLs[19–22]. But γ-M-γ-B, α-M-γ-B-1, and γ-B, which lost the α,β-unsaturated ketone moiety (marked with red in Fig. 1D), have not been independently identified in the structures of anti-inflammatory SLs. This result indicates that the α,β-unsaturated ketone within the conserved α-M-γ-B (marked with red in Fig. 1B) might play a critical role in the anti-inflammatory SLs.

3.2. *Small molecule α-M-γ-B with strong electrophilicity exhibits potent anti-inflammatory activity*

The electrophilic α,β-unsaturated ketone group is a Michael acceptor present in numerous bioactive natural products and clinically relevant therapeutic agents[23]. Dimethyl fumarate which embodied the α,β-unsaturated ketone structure was licensed as an

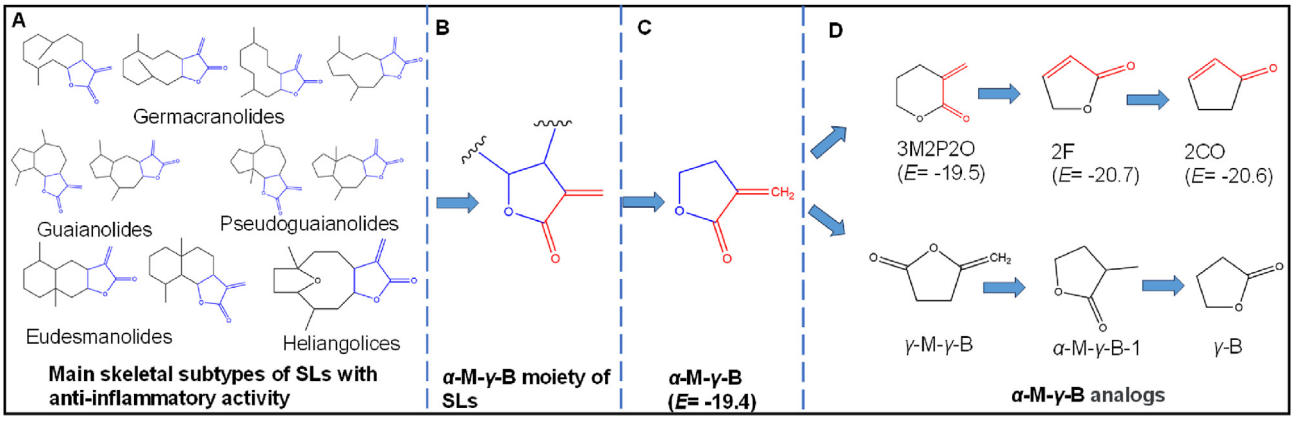

Figure 1 Methylene-γ-butyrolactone (α-M-γ-B) is a conserved moiety in natural sesquiterpene lactones (SLs) with anti-inflammatory activity. (A) Main skeletal subtypes of SLs with anti-inflammatory activity. (B) Conserved α-M-γ-B moiety in anti-inflammatory SLs. (C) SLs-structure-simplified small molecule, α-M-γ-B. (D) Six α-M-γ-B analogs marked with electrophilicity *E*.

anti-inflammatory therapeutic agent for multiple sclerosis in clinic[24]. However, the anti-inflammatory potential of α-M-γ-B, as an independent small molecule, has not been fully demonstrated. Thus, we examined the potential anti-inflammatory effects of α-M-γ-B and its six analogs by evaluating their inhibitory capacities on nitric oxide (NO), a widely used inflammatory marker for assessing the anti-inflammatory properties of SLs[12,25]. As expected, α-M-γ-B, 3M2P2O, 2F and 2CO (except γ-M-γ-B, α-M-γ-B-1, and γ-B) suppressed the production of NO in lipopolysaccharide (LPS)-induced macrophages (Fig. 2A). Among the four effective compounds, α-M-γ-B showed the lowest EC_{50} (half maximal effective concentration) against LPS-induced NO production (Fig. 2A), followed by the order of 3M2P2O < 2CO < 2F. Interestingly, the anti-inflammatory activities of the four molecules are positively relevant to their electrophilicity E (α-M-γ-B, $E = -19.4$; 3M2P2O, $E = -19.5$; 2CO, $E = -20.6$; 2F, $E = -20.7$) reported by Ofial et al.[26]. Due to the loss of α,β-unsaturated ketone moiety, γ-M-γ-B, α-M-γ-B-1, and γ-B exhibited the weakest electrophilicity, as well as the weakest anti-inflammatory activity at the same time. While α-M-γ-B exhibited both the strongest electrophilicity and strongest anti-inflammatory activity.

Therefore, we further evaluated the anti-inflammatory properties and underlying molecular mechanisms of α-M-γ-B. As shown

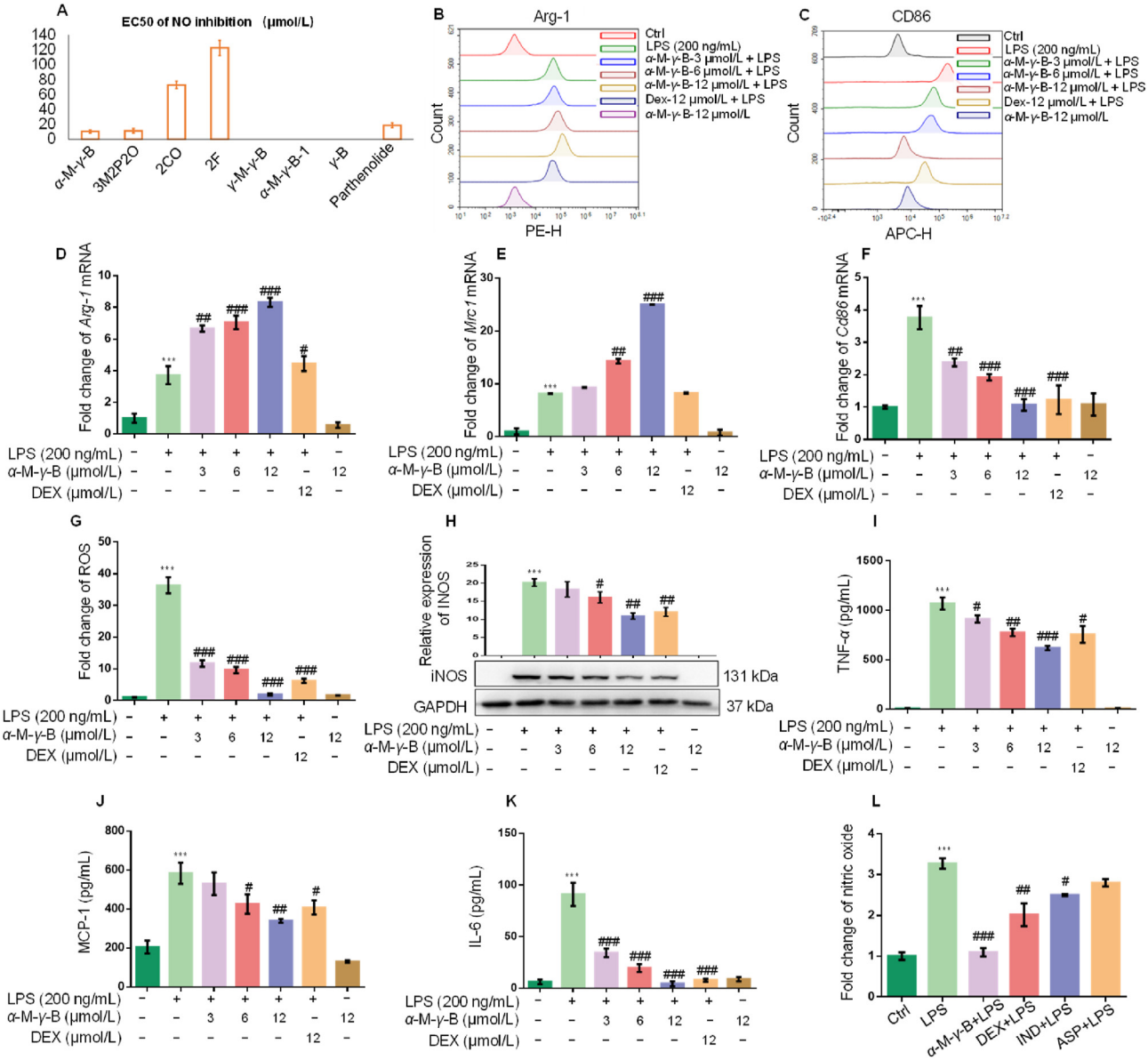

Figure 2 Small molecule α-M-γ-B with strong electrophilicity exhibited potent anti-inflammatory activity. (A) Half maximal effective concentration (EC_{50}) of α-M-γ-B and its structural analogues against LPS-induced NO in RAW264.7 ($n = 6$). (B−C) Flow cytometry was utilized to detect the M1 marker CD86 and M2 marker ARG-1 on the cell surface of RAW264.7 cells ($n = 6$). (D−F) mRNA levels of macrophage-related genes (*Arg-1*, *Mrc1*, *Cd86*), (G) intracellular ROS, (H) the protein expression of iNOS, and (I−K) cytokines in cultural supernatant were detected in LPS-induced RAW264.7 ($n = 6$). (L) The maximum inhibition of α-M-γ-B, dexamethasone (DEX), indomethacin (IND), and aspirin (ASP) against LPS-induced NO in RAW264.7 cells ($n = 6$). $^{***}P < 0.001$ *vs.* the Ctrl, while $^{\#}P < 0.05$, $^{\#\#}P < 0.01$ and $^{\#\#\#}P < 0.001$ *vs.* the LPS.

in Supporting Information Fig. S1A and Fig. 2B−F, under the nontoxic concentrations, α-M-γ-B suppressed the activation of M1 macrophages and promoted the polarization towards M2 in LPS-stimulated RAW264.7 and PMA-differentiated THP-1 cells (Supporting Information Fig. S2A−S2C). Moreover, α-M-γ-B declined the LPS-induced elevation of pro-inflammatory mediators such as NO, iNOS, ROS, IL-1β, IL-6, TNF-α and MCP-1, while it increased the anti-inflammatory cytokine IL-10, in RAW264.7 macrophages (Fig. S1B−S1F and Fig. 2G−K) and PMA-differentiated THP-1 cells (Fig. S2D−S2L). Notably, α-M-γ-B exhibited a superior ability on NO inhibition compared to commonly used NSAIDs (aspirin and indomethacin) and the glucocorticoid dexamethasone (Fig. 2L), indicating its heightened anti-inflammatory potential.

3.3. α-M-γ-B significantly attenuates CII-induced arthritic phenotype in mice

Previously, we demonstrated that Leocarpinolide B (LB), a kind of anti-inflammatory SL that embodied the α-M-γ-B moiety, attenuated the CII-induced arthritic (CIA) phenotype in mice[15]. Other anti-inflammatory SLs, such as budlein A and parthenolide, were also reported to be effective in RA treatment[27−29]. Thus, we evaluated the anti-arthritic effects of α-M-γ-B in CIA mice. Firstly, acute toxicity was evaluated in mice. The results showed that α-M-γ-B was nontoxicity to the mice when the dose was ≤100 mg/kg (Supporting Information Fig. S3). Therefore, we chose the experimental dose (2.5, 5, 10 mg/kg) reference to the LB under the nontoxic doses. From a 19-day constitutive treatment of α-M-γ-B, no noticeable alterations in body mass were observed, suggesting the absence of α-M-γ-B-induced toxicity (Fig. 3A−B). α-M-γ-B attenuated the CIA phenotype, which was characterized by reduced foot swelling and arthritic scores in the CIA mice (Fig. 3C−E). Depicted in the histopathological and radiological images (Fig. 3F−H), the CIA group showed the absence of the articular cavity, replaced by inflammatory infiltration, severe synovial hyperplasia, cartilage defect, and bone erosion. α-M-γ-B administration effectively mitigated the aberrant synovial cell proliferation and moderated the damage to both cartilage and bone. The results showed that α-M-γ-B significantly attenuated CIA phenotype on mice, with comparable effects to the parent structure LB and positive drug dexamethasone (DEX).

3.4. α-M-γ-B significantly restores the balance of regulatory T cells and macrophages in CIA mice

RA is often initiated with an imbalance of T lymphocytes and the release of autoantibodies, which subsequently triggers the polarization of macrophages to produce numerous cytokines, ultimately impacting the synovial cells[30]. Our previous study showed that LB, a kind of anti-inflammatory SL that embodied the α-M-γ-B moiety, had a regulatory effect on $CD4^+FOXP3^+$ T lymphocytes (Tregs), resulting in the function-normalization of macrophages[15]. Results from transcriptome sequencing suggested that α-M-γ-B regulated the immune system pathway (Supporting Information Fig. S4). Thus, we further evaluated the proportion of immune cells in immune organs and autoantibodies levels in the serum of CIA mice. Results from flow cytometry indicated that α-M-γ-B effectively restored the Tregs proportion in the spleen, thymus, and lymph nodes (Fig. 4A−E), α-M-γ-B also modulated the autoantibodies within the normal levels (Fig. 4F and G). Additionally, administration of α-M-γ-B (10 mg/kg) remarkably reduced the serum CRP, IL-17A, IL-6, and IFN-γ in CIA mice (Fig. 4H−K). Moreover, α-M-γ-B (10 mg/kg) was found to effectively decrease mRNA expression of inflammatory cytokines (TNF-α, IL-6, and MCP-1) derived from M1 macrophages in the joint muscle tissue of CIA mice (Fig. 4L−N). These findings suggest that the therapeutic benefits of α-M-γ-B for treating CIA may involve restoring immune function.

3.5. α-M-γ-B improves the synovial microenvironment through modulating synovial-associated macrophages

In the progression of RA, excessively activated macrophages will infiltrate into the synovium, where the macrophage polarization impacts the synovial microenvironment, leading to angiogenesis and the excessive proliferation of fibroblast-like synoviocytes[31]. Therefore, we further investigated the impact of α-M-γ-B on the modulation of macrophages to synovial microenvironment. As shown in Fig. 5A, the pathological observation showed that α-M-γ-B significantly decreased the infiltration of macrophages to synovial tissue, which was consistent with the reduced F4/80 (macrophage marker)-positive cells (Fig. 5B) and mRNA expression of genes including *Adger1* and *Cd68* (Fig. 5E−F). Moreover, α-M-γ-B significantly decreased the M1-like macrophage marker CD86 (Fig. 5C) and increased the M2-like macrophage marker ARG-1 (Fig. 5D and G), resulting in a significant inhibition of synovitis (Fig. 5H−I). H-type vessels in the synovial area marked with the co-localization of CD31 and endomucin (EMCN) were notably decreased by α-M-γ-B treatment (Fig. 5J), indicating a decrease of angiogenesis in the synovium. Additionally, α-M-γ-B decreased MMP3 expression and its co-localization with synovial fibroblast marker Vimentin (Fig. 5K). The above results indicate that α-M-γ-B might improve the synovial microenvironment by modulating the infiltration and polarization of synovial-associated macrophages in synovial tissues.

3.6. α-M-γ-B inhibits the M1 polarization and inflammation via interference NF-κB p65's DNA binding

NF-κB is a canonical signaling implicated in the regulation of M1 macrophage polarization, and its involvement in the modulation of RA has been extensively reported[7,31]. Several SLs were demonstrated to inhibit inflammation and ameliorate RA *via* regulating NF-κB signal pathway[10]. The trans-nucleus of NF-κB and its binding to DNA are the most critical steps in the process of NF-κB activation. Unexpectedly, our results revealed that sulfasalazine (SSZ) (a NF-κB inhibitor through inhibition of IκBα degradation) prevented the trans-nucleus of NF-κB p65, but α-M-γ-B did not reverse LPS-induced IκBα degradation and nucleus entry of NF-κB p65 (Fig. 6A and Supporting Information Fig. S5). Therefore, we further detected the effects of α-M-γ-B on the DNA binding activity (DBA) of NF-κB in the nucleus. Interestingly, the results showed that α-M-γ-B significantly impacted the DBA of NF-κB in macrophages and synovial tissues of CIA mice (Fig. 6B−D). Moreover, ChIP-qPCR demonstrated that α-M-γ-B disrupted the binding of NF-κB p65 to the promoter regions of *NOS2* and *IL6* genes associated with M1 polarization and inflammation (Fig. 6E−F). These results indicate that α-M-γ-B might attenuate RA by interfering with the NF-κB p65's DNA binding to the pro-inflammatory promoters.

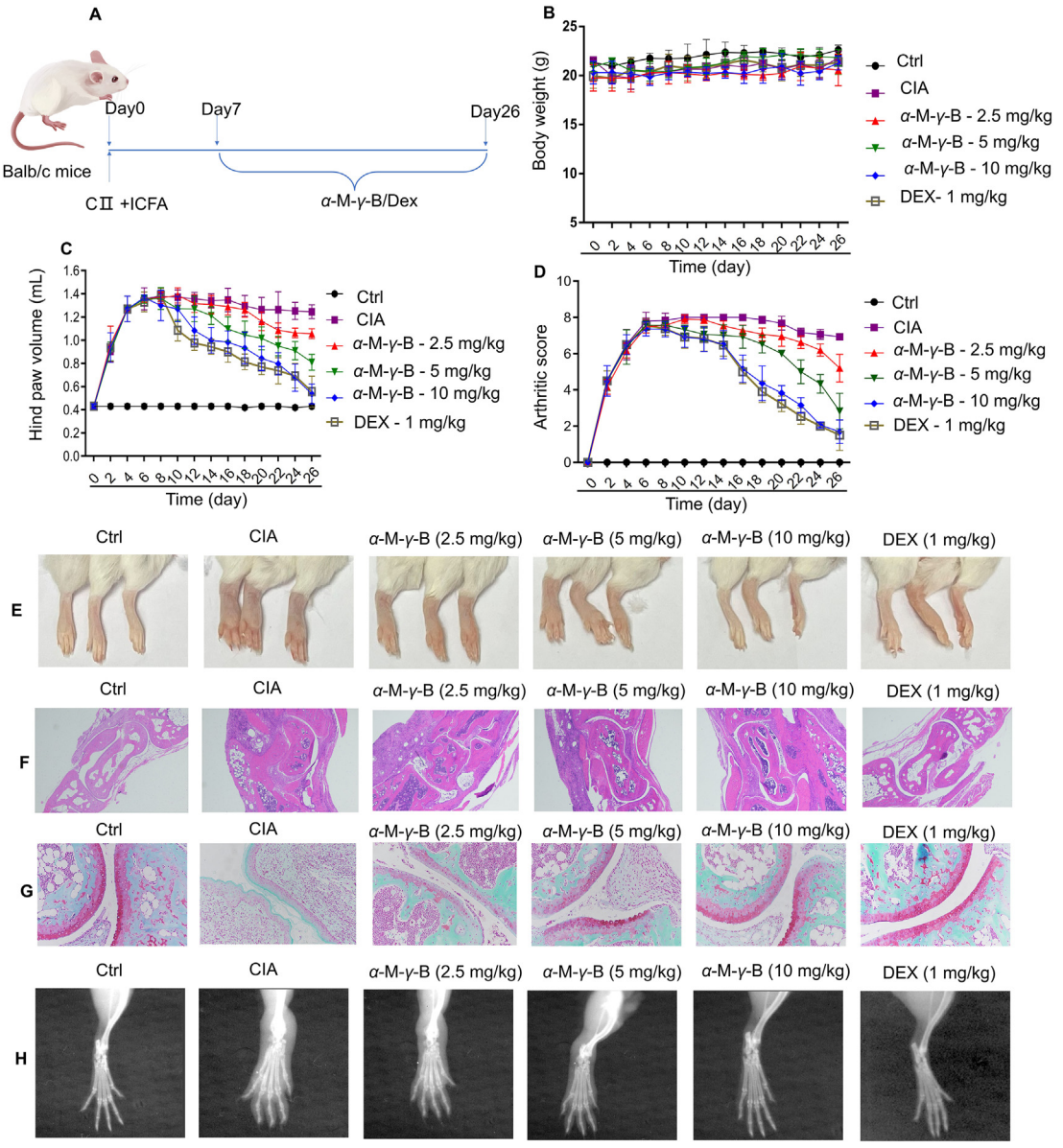

Figure 3 α-M-γ-B significantly attenuated arthritic phenotype in mice. (A) The experimental route on mice. (B) Body weight, (C) Hind paw volume, and (D) Arthritic score were monitored and recorded every 2 days. (E) On the final administration day, photographs were taken to capture representative morphological alterations in the hind paws of mice. (F—G) Pathological changes in joints were assessed with safranin O-fast green staining (original magnification × 20; $n = 5$) and hematoxylin-eosin (H&E) staining (original magnification × 4; $n = 5$). (H) The bone structure of the hind paw was examined by acquiring X-ray images ($n = 5$).

3.7. α-M-γ-B disrupts the DNA binding of NF-κB via direct interaction with NF-κB p65

Our previous study with network pharmacology predicted that the *RELA* gene (responsible for encoding the NF-κB p65) emerged as a highly significant target implicated in both the occurrence and progression of RA[32]. Consistently, several SLs embodied the structure of α-M-γ-B were reported to be anti-inflammation and anti-RA *via* targeting NF-κB p65[15,33]. Molecular docking between α-M-γ-B and IκBα-NF-κB p65-NF-κB p50 protein complex (1NFI) showed that α-M-γ-B preferentially bound to p65, indicating that the binding affinity of α-M-γ-B to p65 is stronger than that of p50 and IκBα (Fig. 7E). Therefore, we hypothesized that α-M-γ-B could exert the therapeutic benefits *via* direct interaction with NF-κB p65 and interference the DBA of NF-κB. The interaction between NF-κB p65 and α-M-γ-B was experimentally confirmed through an isothermal titration calorimetry (ITC) assay, wherein the p65 protein was titrated with α-M-γ-B. The result showed that α-M-γ-B directly bound to NF-κB p65 (Fig. 7A) with a $K_D = 8.47 \pm 0.12$ μmol/L. In the cellular thermal shift assay (CETSA), α-M-γ-B effectively hindered the heat-induced denaturation of NF-κB p65 at various temperatures, resulting in a noticeable shift towards higher temperatures in the melt curves (Fig. 7B).

The NF-κB inhibitors, parthenolide and helenalin, were reported to directly bind to the cysteine residues of NF-κB p65 and disrupt the DBA of NF-κB[34,35]. Of note, α-M-γ-B serves as the primary active centers for both parthenolide and helenalin to target

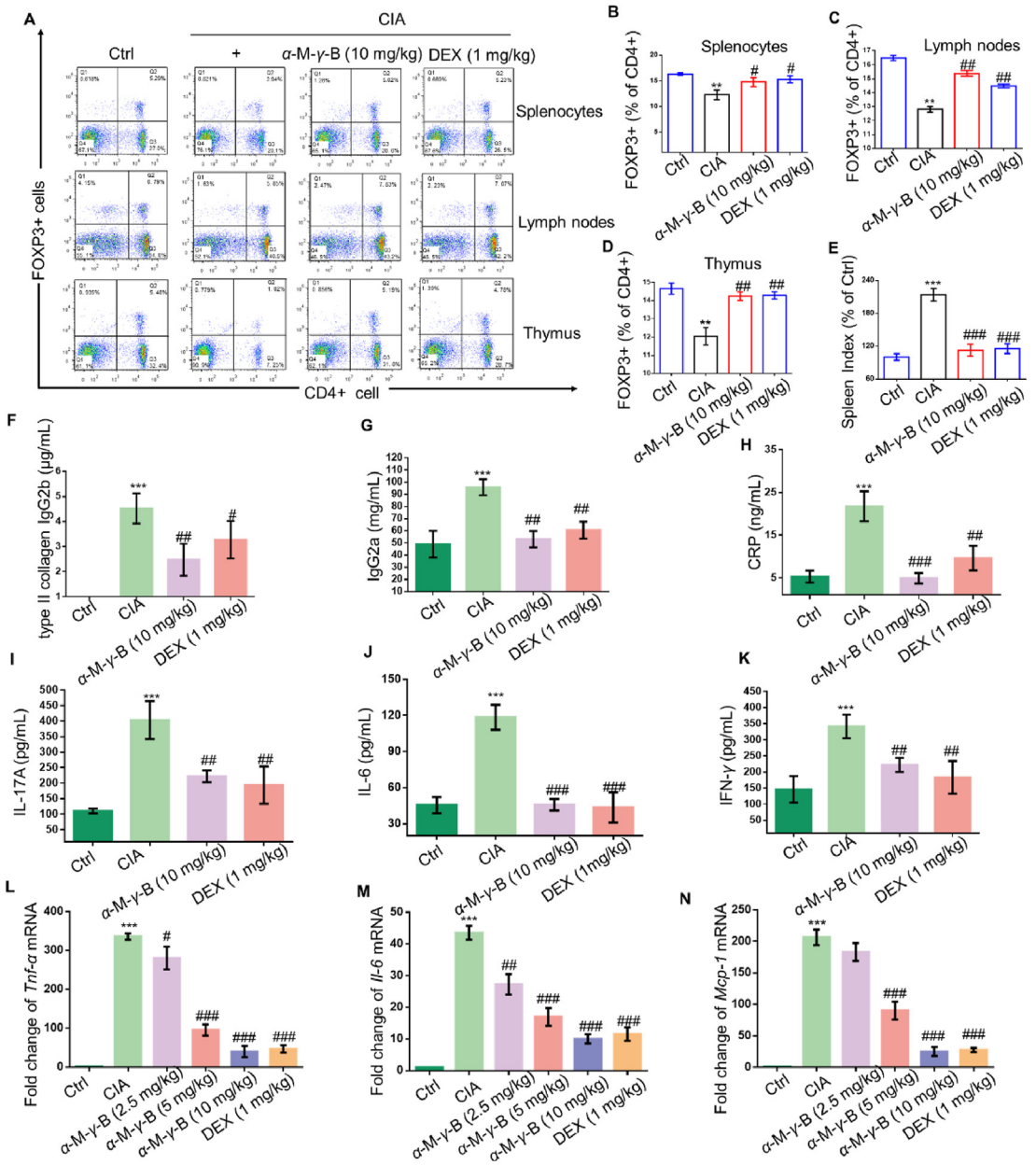

Figure 4 α-M-γ-B significantly restored the balance of Tregs and macrophages in CIA mice. (A) The percentages of $FOXP3^+$ and $CD4^+$ T cells in splenocytes, lymph nodes, and thymus were examined. (B−D) The proportion of $FOXP3^+$ in $CD4^+$ T cells in splenocytes, lymph nodes, and thymus ($n = 5$). (E) The spleen index in different treatment groups ($n = 5$). (F−K) Proteins in serum were determined by ELISA kits ($n = 5$). (L−N) mRNA expression of inflammatory genes in the joint muscles was detected by qPCR ($n = 5$). $^{***}P < 0.001$ *vs.* the Ctrl, while $^{\#}P < 0.05$, $^{\#\#}P < 0.01$ and $^{\#\#\#}P < 0.001$ *vs.* the CIA.

NF-κB p65[26,34]. Thus, we speculated that α-M-γ-B could directly interact with the cysteine residues of NF-κB p65 to initiate anti-inflammatory effects like parthenolide and helenalin. It was confirmed by *N*-acetyl-L-cysteine (NAC) turnover analysis in Fig. 7B that α-M-γ-B could not enhance the thermal stability of NF-κB p65 when the cells were pretreated with α-M-γ-B in the presence of NAC. NAC is a free cysteine that could competitively bind to α-M-γ-B and antagonize the binding of α-M-γ-B to cysteine residues on NF-κB p65. The covalent binding of α-M-γ-B with NAC was confirmed in Fig. 7C, α-M-γ-B also covalently bound with glutathione (GSH) (Fig. 7C), and both NAC and GSH contained the thiol group. These results indicated that electrophilic α-M-γ-B could directly target NF-κB p65 *via* covalent binding on the nucleophilic sulfhydryl (thiol group) of cysteine residues on NF-κB p65. Furthermore, α-M-γ-B failed to disrupt the DBA of NF-κB in the presence of NAC (Fig. 7D). Taken together, these results suggest that α-M-γ-B targets the cysteine sulfhydryl in the p65 subunit of NF-κB, thus interfering the DBA of NF-κB.

3.8. α-M-γ-B loses the anti-arthritic effects in the presence of NAC or on the Ad-sh-Rela mice

Due to the antagonistic characteristics of NAC in interference with the DBA of NF-κB, we further investigated the anti-arthritic

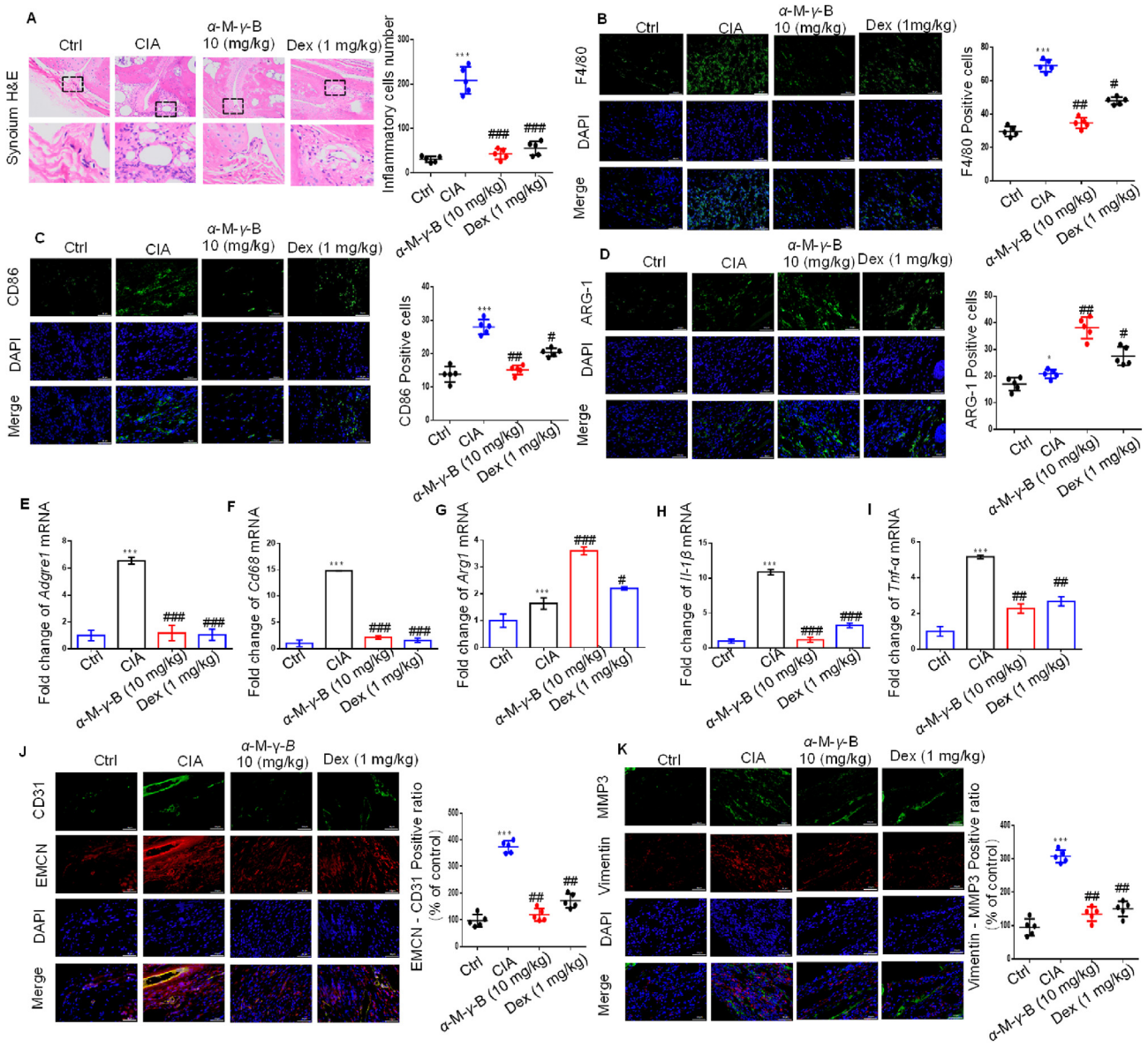

Figure 5 α-M-γ-B improved the synovial microenvironment through modulating synovial-associated macrophages. (A) Inflammatory infiltration of macrophages to synovium was assessed with hematoxylin-eosin (H&E) staining (original magnification × 20; $n = 5$). (B) Total macrophage markers F4/80, (C) CD86, and (D) ARG-1 were assessed by immunofluorescence staining ($n = 5$). (E−I) mRNA levels of genes in the synovial tissue were assessed by qPCR ($n = 5$). (J−K) Representative immunofluorescent images of positive Vimentin, MMP3, CD31, and EMCN, and quantification analysis in the synovial tissues ($n = 5$). $^{***}P < 0.001$ *vs.* the Ctrl, while $^{\#}P < 0.05$, $^{\#\#}P < 0.01$ and $^{\#\#\#}P < 0.001$ *vs.* the CIA. Scale bar = 50 μm.

effects of α-M-γ-B in the presence of NAC. As shown in Fig. 8A−D and Supporting Information Fig. S6A−S6B, α-M-γ-B failed to inhibit the polarization of M1 macrophages and the production of inflammatory mediators in LPS-activated macrophages in the presence of NAC, suggesting that α-M-γ-B lost the anti-inflammatory capacity in the presence of NAC. To simulate the impact of synovial-associated macrophages on the synovial microenvironment, we used the macrophage-conditioned medium (from LPS-activated THP-1 macrophages) to treat the synovial cells and detect the arthritic phenotype of synovial cells. As shown in Fig. 8E−F and Fig. S6C−S6D, both α-M-γ-B and SSZ significantly inhibited the proliferation, migration, and invasion of synovial cells induced by macrophage conditioned-medium, the effects of α-M-γ-B but not SSZ were reversed by NAC. Also, NAC reversed the effects of α-M-γ-B on the monocyte adhesion to synovial cells (Fig. 8G−H) and angiogenesis of HUVECs (Fig. 8I−J), but NAC did not impact the effects triggered by SSZ.

Therefore, we investigated the anti-arthritic effects of α-M-γ-B in the presence of NAC or on the Ad-sh-*Rela* mice (mice subjected to the macrophage-specific deficiency of *Rela*), the results showed that co-treatment of NAC and α-M-γ-B failed to attenuate the arthritic phenotype (Fig. 8K−L) in CIA mice. Importantly, no additive protection effects were observed when CII and ICFA-challenged Ad-sh-*Rela* mice were treated with α-M-γ-B (Fig. S6E−S6F and Fig. 8K−L). α-M-γ-B also lost the function of reducing M1 polarization and inhibiting the DBA of NF-κB in the presence of NAC or on the Ad-sh-*Rela* mice (Fig. S6G−S6H). Taken together, α-M-γ-B attenuated arthritic phenotype by

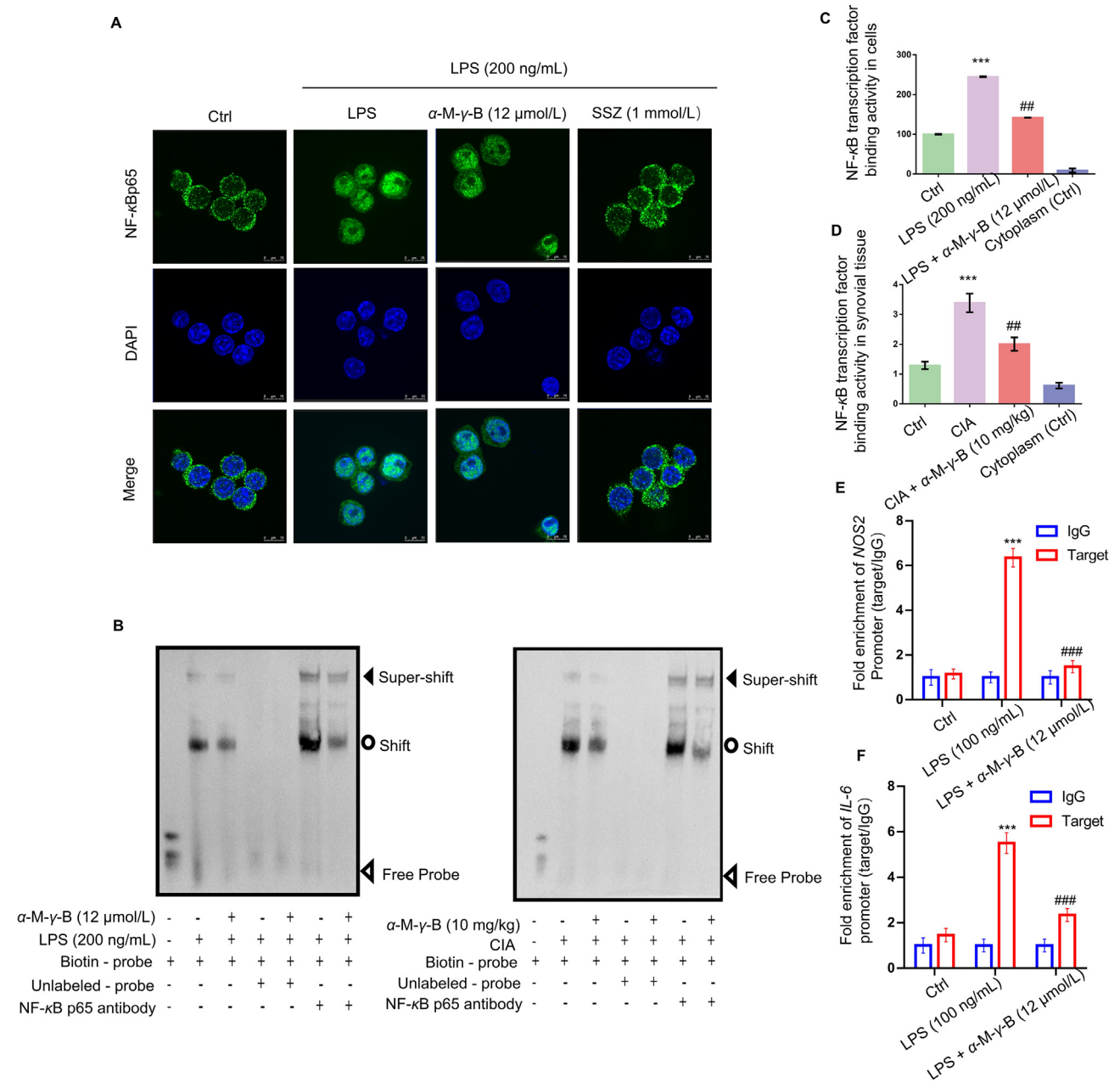

Figure 6 α-M-γ-B inhibited the M1 polarization and inflammation *via* interference DBA of NF-κB. (A) Sulfasalazine (SSZ) but not the α-M-γ-B prevented LPS-stimulated trans-nucleus of p65 in RAW264.7 ($n = 5$). (B) Electrophoretic mobility shift assay revealed that α-M-γ-B inhibited the NF-κB p65's DNA binding in LPS-stimulated macrophages and CIA synovial tissues ($n = 5$). (C−D) Results from the transcription factor assay kit indicated that α-M-γ-B inhibited DBA of NF-κB in LPS-stimulated macrophages and CIA synovial tissue ($n = 5$). (E−F) Chromatin immunoprecipitation (ChIP)-qPCR suggested that α-M-γ-B interfered with the DNA binding of p65 to promoter area of *IL6* and *NOS2* genes in LPS-stimulated THP-1 macrophages ($n = 5$). $^{***}P < 0.001$ *vs.* the Ctrl, while $^{\#\#}P < 0.01$ and $^{\#\#\#}P < 0.001$ *vs.* the model (LPS or CIA). Scale bar = 10 μm.

targeting the cysteine residue in NF-κB p65, which could be counteracted by the antagonist NAC and deficiency of NF-κB p65.

4. Discussion

The pathogenesis of RA involves persistent autoimmune inflammation, hyperplasia of synovial tissue, and progressive degradation of cartilage and bone. Irreversible destruction of cartilage and bone may even cause deformities and serious complications[1], which seriously affects people's health and life quality. Currently employed conventional medications (such as NSAIDs, DMARDs, and glucocorticoids) could not cure RA completely or be linked with significant adverse effects[3,8]. Natural products have emerged as a promising alternative for the discovery of drug leads, owing to their efficacy and safety.

SLs are likely the most abundant group of plant secondary metabolites, with more than 5000 structures documented so far[9−12]. They are identified as the bioactive components of various

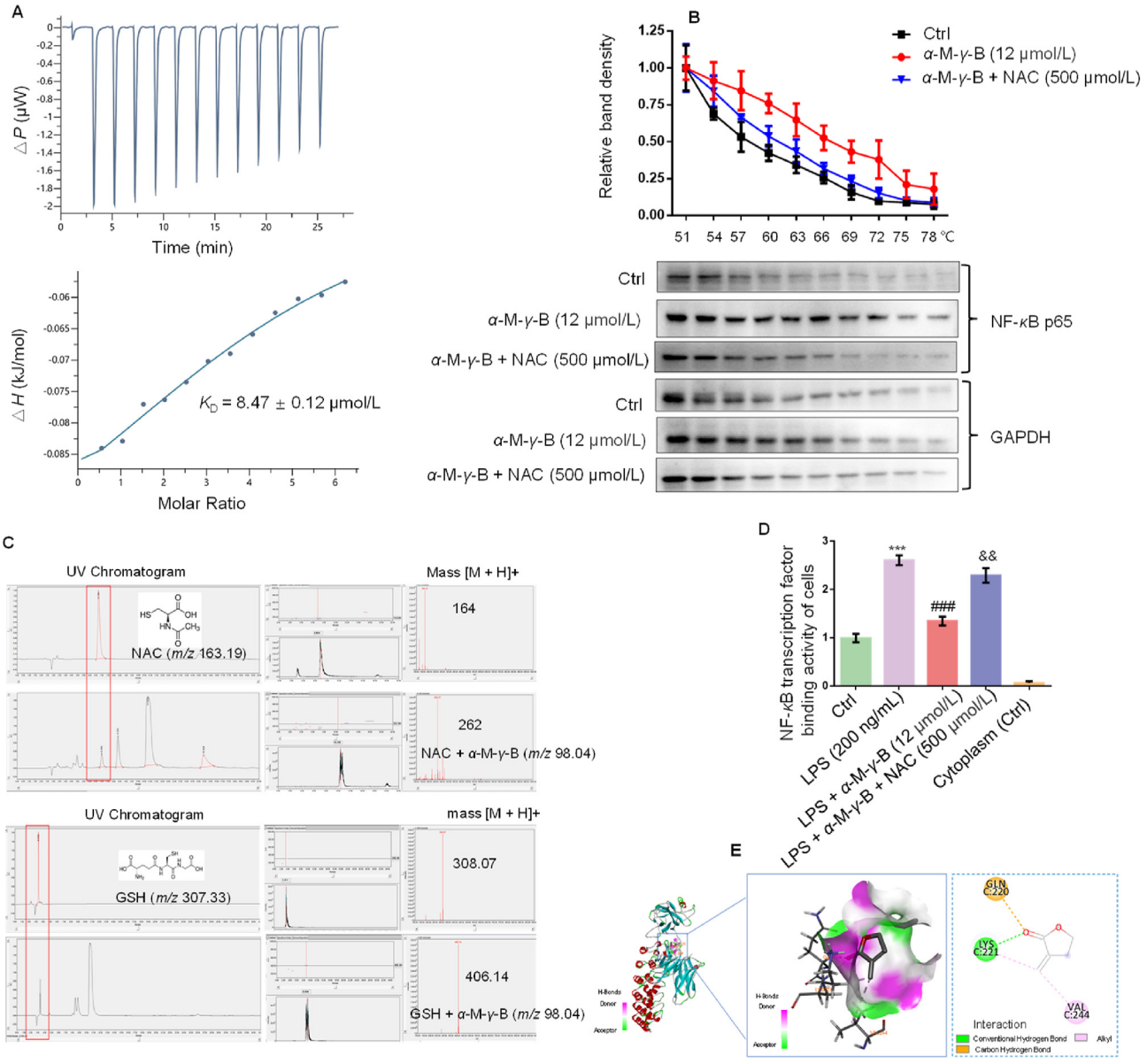

Figure 7 α-M-γ-B disrupts the DBA of NF-κB *via* direct interaction with NF-κB p65. (A) Isothermal titration calorimetry assay revealed that α-M-γ-B exhibited a binding affinity towards recombinant human p65 protein, with a measured binding constant $K_D = 8.47 \pm 0.12$ μmol/L. (B) Interaction between α-M-γ-B and p65 was demonstrated by cellular thermal shift assay. (C) Covalent binding between α-M-γ-B and *N*-acetylcysteine (NAC) or glutathione (GSH) was identified with UPLC−MS. (D) Results from the transcription factor assay kit indicated that α-M-γ-B failed to inhibit the DBA of NF-κB in the presence of the NAC in LPS-stimulated macrophages ($n = 5$). (E) Molecular docking between α-M-γ-B and IκBα-NF-κB p65-NF-κB p50 protein complex (1NFI) indicated a direct binding between α-M-γ-B and NF-κB p65. $^{***}P < 0.001$ *vs.* the Ctrl, $^{\#\#\#}P < 0.001$ *vs.* the LPS and $^{\&\&}P < 0.01$ *vs.* the α-M-γ-B + LPS.

medicinal plants utilized in traditional medicine for managing inflammatory disorders[10,15]. There are several skeletal subtypes, mainly including germacranolides, guaianolides, eudesmanolides, heliangolides, pseudoguaianolides, and hypocretenolides. Interestingly, almost all anti-inflammatory SLs embodied a conserved α-methylene-γ-butyrolactone (α-M-γ-B) moiety. However, it is unknown why this moiety was chosen to be conserved in the anti-inflammatory SLs, it is also unknown about the anti-arthritic potentials when the α-M-γ-B is an independent small molecule.

Therefore, we obtained the SLs-structure-simplified small molecule α-M-γ-B, which is a natural compound (also called Tulipalin A) with a well-established chemical synthesis route[36]. Then, we demonstrated its anti-inflammatory effects *via* repolarization RAW264.7 and THP-1 macrophages. Of note, α-M-γ-B exhibited a superior ability on NO inhibition compared to commonly used NSAIDs (aspirin and indomethacin) and the glucocorticoid dexamethasone, indicating its heightened anti-inflammatory efficacy. Additionally, α-M-γ-B restored the imbalance of regulatory T lymphocytes-macrophages and remodeled the synovial microenvironment by modulating the infiltration and polarization of synovial-associated macrophages in synovial tissue, which inhibited the angiogenesis of vascular endothelial cells and excessive proliferation of fibroblast-like synoviocytes thus attenuated the arthritic phenotype in CIA mice.

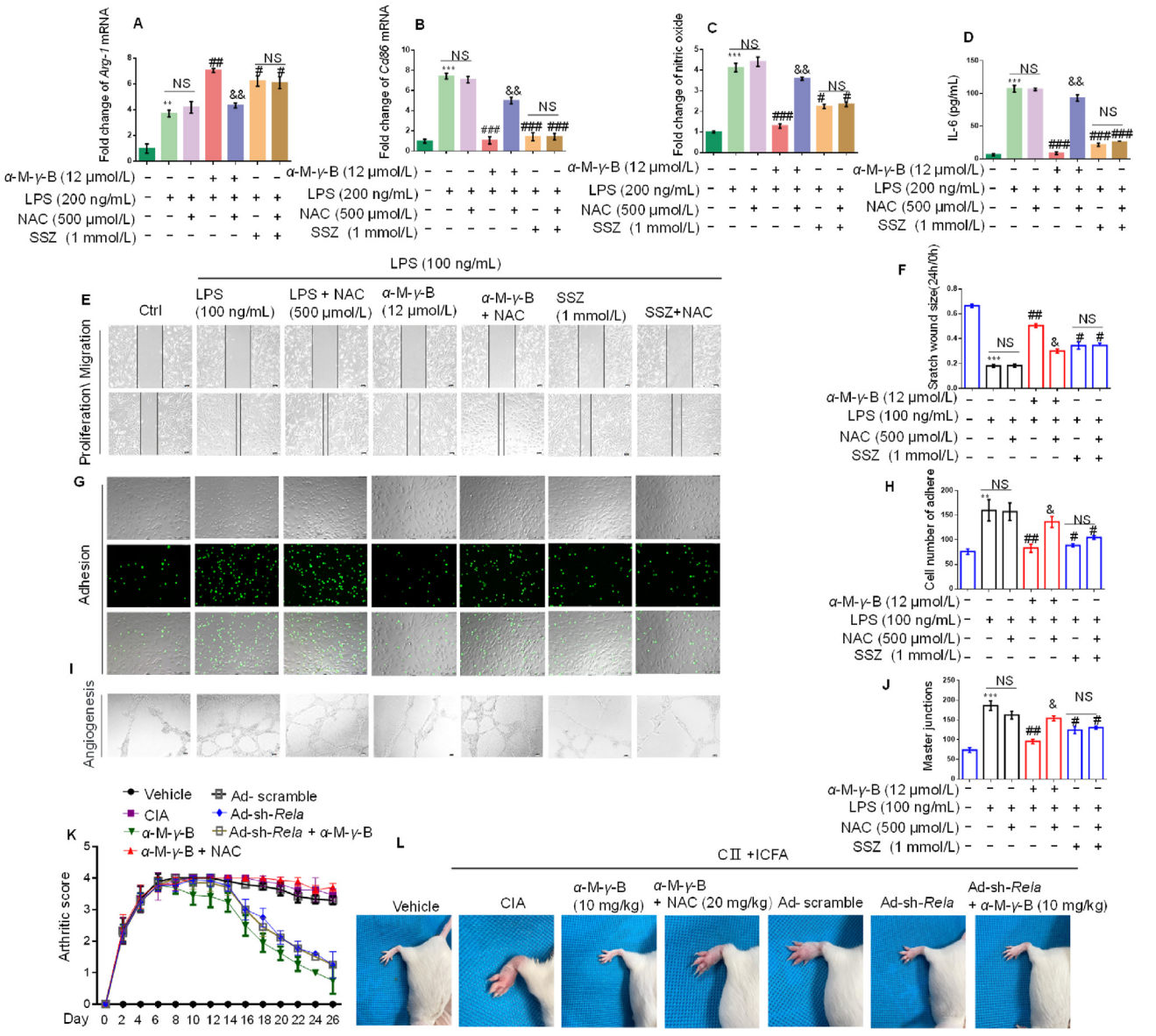

Figure 8 α-M-γ-B lost the anti-arthritic effects in the presence of NAC or on the Ad-sh-*Rela* mice (mice subjected to the macrophage-specific deficiency of *Rela*). (A—D) NAC reversed the α-M-γ-B-mediated increase of *Arg*-1 mRNA and decrease of *Cd8*6 mRNA, also limited the inhibitory effect of α-M-γ-B on LPS-induced NO and IL-6 in RAW264.7 macrophages ($n = 6$). (E—F) NAC abrogated the action of α-M-γ-B on inhibiting the proliferation and migration of synovial SW982 cells induced by macrophage-conditioned medium (the THP-1 macrophages were exposed to α-M-γ-B along with or without 100 ng/mL LPS for a duration of 12 h, then the supernatant was harvested as macrophage conditioned media). Scale bar = 50 μm. (G—H) The inhibitory effect of α-M-γ-B on the adhesion of THP-1 monocytes (pre-stained with BCECF/AM) to synovial SW982 cells induced by macrophage conditioned-medium was counteracted by NAC. Scale bar = 100 μm. (I—J) NAC abrogated the action of α-M-γ-B on inhibiting the angiogenesis of HUVECs induced by a macrophage-conditioned conditioned-medium. Scale bar = 50 μm. (K—L) α-M-γ-B lost the anti-arthritic effects on the Ad-sh-*Rela* mice (mice were subjected to the macrophage-specific deficiency of *Rela*). To establish the macrophage-specific knockdown of NF-κB p65 (*Rela*) in mice, the adeno-associated virus (AAV) vector with the macrophage-specific promoter F4/80-mediated knockdown of mouse *Rela* (Ad-sh-*Rela*) and control (Ad-*scramble*) were constructed and injected into the mice for 30 days. Then, the arthritic model was replicated by subcutaneous injection of CII emulsified in ICFA. On Day 7 of the first immunization, the mice received intraperitoneal injections of saline or drugs once daily. The arthritic score was determined every other day, and the representative hind paw morphologies of mice were photographed at the end of the experiment ($n = 6$). $^{***}P < 0.001$ *vs.* the Ctrl, $^{\#}P < 0.05$, $^{\#\#}P < 0.01$ and $^{\#\#\#}P < 0.001$ *vs.* the LPS, while $^{\&\&}P < 0.01$ and $^{\&}P < 0.05$ *vs.* the α-M-γ-B + LPS.

Different from the NF-κB inhibitor sulfasalazine which prevented the trans-nucleus of NF-κB through inhibiting IκBα degradation, α-M-γ-B did not impact the IκBα degradation and trans-nucleus of NF-κB p65. Inspired by the anti-inflammatory mechanisms of commercial NF-κB inhibitors (parthenolide and helenalin) through targeting NF-κB p65[34,35], we further revealed the underlying anti-inflammatory and anti-arthritic mechanisms of α-M-γ-B. Specifically, electrophilic α-M-γ-B was demonstrated to interfere DBA of NF-κB by forming a covalent bond with the nucleophilic sulfhydryl (thiol group) of cysteine residues on NF-

κB p65, thus inhibiting the NF-κB-mediated M1 polarization and pro-inflammatory mediators. The anti-arthritic capacity of α-M-γ-B was reversed in the presence of NAC which could competitively antagonize the binding of α-M-γ-B to cysteine residues on NF-κB p65. Importantly, α-M-γ-B could not alter additive protection effects when the mice were subjected to a macrophage-specific deficiency of *Rela*. Previously, Merfort et al. investigated a set of 103 different SLs (almost all embodied the α-M-γ-B moiety) and revealed their inhibition on DBA of NF-κB[33]. Taken together, these results suggest the anti-inflammatory contribution of α-M-γ-B moiety widely existed in anti-inflammatory SLs, and α-M-γ-B is a potential anti-inflammatory and anti-arthritic candidate *via* direct targeting to NF-κB p65 and interfering with the DBA of NF-κB.

Previously reported data from different research groups and our earlier results predict that the SLs bind to the target protein through electrophilic addition to exert an anti-inflammatory effect[10]. However, there is no direct evidence for an equivalence relationship between the anti-inflammatory activity and electrophilicity of SLs. In the present study, we made an anti-inflammatory comparison among the α-M-γ-B and six analogs including 3-methylenetetrahydro-2*H*-pyran-2-one (3M2P2O), 2(5*H*)-furanone (2F), 2-cyclopenten-1-one (2CO), γ-methylene-γ-butyrolactone (γ-M-γ-B), α-methyl-γ-butyrolactone (α-M-γ-B-1) and γ-butyrolactone (γ-B). Interestingly, their electrophilicity E (α-M-γ-B, $E = -19.4$; 3M2P2O, $E = -19.5$; 2CO, $E = -20.6$; 2F, $E = -20.7$) was detected and reported by Ofial et al.[26]. Therefore, we can conclude that the electrophilicity of SLs is positively correlated with the anti-inflammatory activity obtained from our present experiments. α-M-γ-B exhibited both the strongest anti-inflammatory activity and strongest electrophilicity. Plants might have chosen the strongest electrophilicity α-M-γ-B as the most abundant fragment in anti-inflammatory SLs because the cyclic scaffold of α-M-γ-B can be utilized to incorporate stereochemical information in living organisms[26].

In addition, Ofial et al. proposed that the electrophilic capacity of α-M-γ-B is comparable to that of naturally occurring SLs with the α-M-γ-B structure, such as parthenolide, costunolide, dehydroleucodine, and dehydrocostus lactone[26]. Consistently, our results showed that both α-M-γ-B and parthenolide exhibited similar EC_{50} on NO inhibition (Fig. 2A) and therapeutic effects on CIA based on the reported data[28,29]. Liang et al. reported that costunolide and α-M-γ-B exhibited similar inhibition on IL-1β[37]. From this perspective, α-M-γ-B is deemed to be a potential alternative molecule for most natural SLs, especially those natural SL compounds that are low in content and difficult to synthesize. If researchers focusing on natural SLs are aware of the alternative possibility of α-M-γ-B and compare the anti-inflammatory effects of SLs they are undertaking with α-M-γ-B before conducting follow-up research, it is possible to help them avoid the waste of research resources. Prospectively, it would be a good research direction to carry out structural modification based on the structure of α-M-γ-B and find safer and more effective α-M-γ-B derivatives for managing inflammatory disorders.

Acknowledgments

Financial support by the National Natural Science Foundation of China (82260801), China Postdoctoral Science Foundation (2023M730815, China), Excellent Young Talents Plan of Guizhou Medical University (2023110, China), the Guizhou Provincial Scientific and Technologic Innovation Base ([2023]003, China), the High Level Innovation Talents (GCC[2023]048, China), Science and Technology Development Fund, Macau SAR (0159/2020/A3, China), Guizhou Provincial Science and Technology Project (ZK[2024]152, China) and Guizhou Provincial Health Commission Science and Technology Foundation (gzwkj2023-153, China) are gratefully acknowledged.

Author contributions

Kegang Linghu, Xiangchun Shen and Haiyang Li designed the study; Kegang Linghu, Wenqing Cui, Taiqin Li and Yueting Tuo performed and analyzed the biological experiments; Huiqi Pan and Dasong Wang performed the literature summary and drew the chemical structures; Tian Zhang and Xiaoxia Hu helped on the animal experiments; Kegang Linghu, Wenqing Cui and Xiaoxia Hu wrote the manuscript; Ligen Lin and Hua Yu guided the chemical analysis.

Conflicts of interest

The authors have declared that no competing interest exists.

Appendix A. Supporting information

Supporting information to this article can be found online at https://doi.org/10.1016/j.apsb.2024.04.004.

References

1. Alivernini S, Firestein GS, McInnes IB. The pathogenesis of rheumatoid arthritis. *Immunity* 2022;**55**:2255–70.
2. Scherer HU, Häupl T, Burmester GR. The etiology of rheumatoid arthritis. *J Autoimmun* 2020;**110**:102400.
3. Radu AF, Bungau SG. Management of rheumatoid arthritis: an overview. *Cells* 2021;**10**:2857.
4. Aungier SR, Cartwright AJ, Schwenzer A, Marshall JL, Dyson MR, Slavny P, et al. Targeting early changes in the synovial microenvironment: a new class of immunomodulatory therapy?. *Ann Rheum Dis* 2019;**78**:186–91.
5. Buckley CD, Ospelt C, Gay S, Midwood KS. Location, location, location: how the tissue microenvironment affects inflammation in RA. *Nat Rev Rheumatol* 2021;**17**:195–212.
6. Fukui S, Iwamoto N, Takatani A, Igawa T, Shimizu T, Umeda M, et al. M1 and M2 monocytes in rheumatoid arthritis: a contribution of imbalance of M1/M2 monocytes to osteoclastogenesis. *Front Immunol* 2018;**8**:195.
7. Han C, Yang Y, Sheng Y, Wang J, Zhou X, Li W, et al. Glaucocalyxin B inhibits cartilage inflammatory injury in rheumatoid arthritis by regulating M1 polarization of synovial macrophages through NF-κB pathway. *Aging (Albany NY)* 2021;**13**:22544–55.
8. Cronstein BN, Aune TM. Methotrexate and its mechanisms of action in inflammatory arthritis. *Nat Rev Rheumatol* 2020;**16**:145–54.
9. Paço A, Brás T, Santos JO, Sampaio P, Gomes AC, Duarte MF. Anti-inflammatory and immunoregulatory action of sesquiterpene lactones. *Molecules* 2022;**27**:1142.
10. Matos MS, Anastácio JD, Dos Santos CN. Sesquiterpene lactones: promising natural compounds to fight inflammation. *Pharmaceutics* 2021;**13**:991.
11. Hohmann MSN, Longhi-Balbinot DT, Guazelli CFS, Navarro SA, Zarpelon AC, Casagrande R, et al. Chapter 7—Sesquiterpene lactones: structural diversity and perspectives as anti-inflammatory molecules. In: Atta-ur-Rahman, editor. *Studies in natural products chemistry*. Elsevier; 2016. p. 243–64.

12. Ivanescu B, Miron A, Corciova A. Sesquiterpene lactones from Artemisia genus: biological activities and methods of analysis. *J Anal Methods Chem* 2015;**2015**:247685.
13. Lyss G, Schmidt TJ, Merfort I, Pahl HL. Helenalin, an anti-inflammatory sesquiterpene lactone from Arnica, selectively inhibits transcription factor NF-κB. *Biol Chem* 1997;**378**:951−61.
14. Linghu KG, Ma QS, Zhao GD, Xiong W, Lin L, Zhang QW, et al. Leocarpinolide B attenuates LPS-induced inflammation on RAW264.7 macrophages by mediating NF-κB and Nrf2 pathways. *Eur J Pharmacol* 2020;**868**:172854.
15. Linghu KG, Zhao GD, Zhang DY, Xiong SH, Wu GP, Shen LY, et al. Leocarpinolide B attenuates collagen type II-induced arthritis by inhibiting DNA binding activity of NF-κB. *Molecules* 2023;**28**:4241.
16. Zhou Y, Gao C, Vong CT, Tao H, Li H, Wang S, et al. Rhein regulates redox-mediated activation of NLRP3 inflammasomes in intestinal inflammation through macrophage-activated crosstalk. *Br J Pharmacol* 2022;**179**:1978−97.
17. Linghu KG, Zhang T, Zhang GT, Lv P, Zhang WJ, Zhao GD, et al. Small molecule deoxynyboquinone triggers alkylation and ubiquitination of Keap1 at Cys489 on Kelch domain for Nrf2 activation and inflammatory therapy. *J Pharm Anal* 2024;**14**:403−17.
18. Linghu KG, Xiong SH, Zhao GD, Zhang T, Xiong W, Zhao M, et al. *Sigesbeckia orientalis* L. extract alleviated the collagen type II-induced arthritis through inhibiting multi-target-mediated synovial hyperplasia and inflammation. *Front Pharmacol* 2020;**11**:547913.
19. Zhou X, Chen X, Cheng X, Lin L, Quan S, Li S, et al. Paeoniflorin, ferulic acid, and atractylenolide III improved LPS-induced neuroinflammation of BV2 microglia cells by enhancing autophagy. *J Pharmacol Sci* 2023;**152**:151−61.
20. Hou J, Dong H, Yan M, Zhu F, Zhang X, Wang H, et al. New guaiane sesquiterpenes from *Artemisia rupestris* and their inhibitory effects on nitric oxide production. *Bioorg Med Chem Lett* 2014;**24**:4435−8.
21. Chen J, Lin X, He J, Liu D, He L, Zhang M, et al. Artemisitene suppresses rheumatoid arthritis progression *via* modulating METTL3-mediated N6-methyladenosine modification of ICAM2 mRNA in fibroblast-like synoviocytes. *Clin Transl Med* 2022;**12**:e1148.
22. Hua L, Liang S, Zhou Y, Wu X, Cai H, Liu Z, et al. Artemisinin-derived artemisitene blocks ROS-mediated NLRP3 inflammasome and alleviates ulcerative colitis. *Int Immunopharm* 2022;**113**:109431.
23. Jackson PA, Widen JC, Harki DA, Brummond KM. Covalent modifiers: a chemical perspective on the reactivity of α,β-unsaturated carbonyls with thiols *via* hetero-Michael addition reactions. *J Med Chem* 2017;**60**:839−85.
24. Xu Z, Zhang F, Sun F, Gu K, Dong S, He D. Dimethyl fumarate for multiple sclerosis. *Cochrane Database Syst Rev* 2015;**2015**:CD011076.
25. Valério DAR, Cunha TM, Arakawa NS, Lemos HP, Da Costa FB, Parada CA, et al. Anti-inflammatory and analgesic effects of the sesquiterpene lactone budlein A in mice: inhibition of cytokine production-dependent mechanism. *Eur J Pharmacol* 2007;**562**:155−63.
26. Mayer RJ, Allihn PWA, Hampel N, Mayer P, Sieber SA, Ofial AR. Electrophilic reactivities of cyclic enones and α,β-unsaturated lactones. *Chem Sci* 2021;**12**:4850−65.
27. Zarpelon AC, Fattori V, Souto FO, Pinto LG, Pinho-Ribeiro FA, Ruiz-Miyazawa KW, et al. The Sesquiterpene lactone, budlein A, inhibits antigen-induced arthritis in mice: role of NF-κB and cytokines. *Inflammation* 2017;**40**:2020−32.
28. Liu Q, Zhao J, Tan R, Zhou H, Lin Z, Zheng M, et al. Parthenolide inhibits pro-inflammatory cytokine production and exhibits protective effects on progression of collagen-induced arthritis in a rat model. *Scand J Rheumatol* 2015;**44**:182−91.
29. Williams B, Lees F, Tsangari H, Hutchinson MR, Perilli E, Crotti TN. Assessing the effects of parthenolide on inflammation, bone loss, and glial cells within a collagen antibody-induced arthritis mouse model. *Mediat Inflamm* 2020;**2020**:6245798.
30. Weyand CM, Goronzy JJ. The immunology of rheumatoid arthritis. *Nat Immunol* 2021;**22**:10−8.
31. Tardito S, Martinelli G, Soldano S, Paolino S, Pacini G, Patane M, et al. Macrophage M1/M2 polarization and rheumatoid arthritis: a systematic review. *Autoimmun Rev* 2019;**18**:102397.
32. Wang Z, Linghu KG, Hu Y, Zuo H, Yi H, Xiong SH, et al. Deciphering the pharmacological mechanisms of the Huayu-Qiangshen-Tongbi formula through integrating network pharmacology and *in vitro* pharmacological investigation. *Front Pharmacol* 2019;**10**:1065.
33. Siedle B, García-Piñeres AJ, Murillo R, Schulte-Mönting J, Castro V, Rüngeler P, et al. Quantitative structure−activity relationship of sesquiterpene lactones as inhibitors of the transcription factor NF-κB. *J Med Chem* 2004;**47**:6042−54.
34. Lyß G, Knorre A, Thomas J, Pahl HL, Merfort I, Schmidt TJ. The anti-inflammatory sesquiterpene lactone helenalin inhibits the transcription factor NF-kappaB by directly targeting p65. *J Biol Chem* 1998;**273**:33508−16.
35. Mathema VB, Koh YS, Thakuri BC, Sillanpää M. Parthenolide, a sesquiterpene lactone, expresses multiple anti-cancer and anti-inflammatory activities. *Inflammation* 2012;**35**:560−5.
36. Kitson RRA, Millemaggi A, Taylor RJK. The renaissance of α-methylene-γ-butyrolactones: new synthetic approaches. *Angew Chem Int Ed* 2009;**48**:9426−51.
37. Xu H, Chen J, Chen P, Li W, Shao J, Hong S, et al. Costunolide covalently targets NACHT domain of NLRP3 to inhibit inflammasome activation and alleviate NLRP3-driven inflammatory diseases. *Acta Pharm Sin B* 2023;**13**:678−93.